Direct visualization of the oscillation of Au (111) surface atoms

T. Hesjedal,[a] E. Chilla, and H.-J. Fröhlich
Paul-Drude-Institut für Festkörperelektronik, Hausvogteiplatz 5-7, D-10117 Berlin, Germany

(Received 14 February 1996; accepted for publication 7 May 1996)

A high frequency oscillating Au (111) surface was measured with atomic resolution using a modified scanning tunneling microscope. On the atomic scale propagating surface acoustic waves lead to oscillations of atoms on elliptical trajectories, with the axes being determined by the material parameters of the surface. Since those oscillation frequencies are much higher than the scan frequencies the topography contrast is reduced. This basic problem is solved by measuring a stroboscopic snapshot seeing a defined state of oscillation. The atomic resolution of the phase and the amplitude contrast is explained by the superposition of the surface topography and the oscillation trajectory. © *1996 American Institute of Physics.* [S0003-6951(96)02529-6]

The measurement of atomic scale features on surfaces of solids has been a great challenge in surface physics since the invention of high resolution scanning tunneling microscopy (STM).[1] A lot of effort must be devoted to vibration isolation in order to obtain atomic resolution. Even periodic surface oscillations due to acoustic waves reduce the STM contrast drastically.[2] Despite such averaging effects the consequences for scanning probe methods resulting from atom or molecule movements due to thermal or high-frequency field excitation are of great interest. Frequency spectra were recorded with an ac-STM in order to investigate organic compounds being adsorbed on a substrate.[3] There are open questions in the field of the dynamical behavior of oscillating molecules,[4] too, like self-assembled monolayer sensor devices.

In order to undergo the electronic problems of measuring high-frequency phenomena at surfaces by STM, we have employed a mixing technique at the nonlinearity of the tunneling curve where the wave information is transferred to STM-electronics compatible frequencies of some 10 kHz. Recently, with this scanning acoustic tunneling microscope (SATM) we measured structural details of nm size on surfaces with propagating surface acoustic waves (SAWs).[5] Other ways of introducing mechanical dynamics to the tip-sample interaction region is, e.g., an ultrasound transducer glued on the backside of the sample[6] or the reverse situation, where a tip vibrating perpendicular to the surface excites waves in the sample by the periodically varying interaction force,[7] or periodically deforming the interaction area due to locally strong rf fields between tip and sample.

There is a tendency for dynamical application of scanning force microscopes (SFMs), too, like the scanning acoustic force microscope (SAFM) where a SAW field is mapped utilizing the nonlinear force curve leading to different tip positions depending on the wave amplitude[8] or the ultrasonic force microscope (UFM)[9] where the point elasticity is mapped through the different dynamic elasticities acting between the microscope's tip and different sample areas. The aim of such types of microscopes is to study the dynamical behavior of surfaces in order to map the elastic properties and at least calculating the elastic constants with high lateral resolution. Furthermore, a deeper understanding of the interacting forces between the tip and the surface is possible since the deflection of the tip is not only distance dependent, but also reflects the relative velocity dependent viscous-type forces.

In this letter we present first measurements on single atoms of a Au (111) surface oscillating on elliptical trajectories as they are excited by propagating Rayleigh-type SAWs. We demonstrate that the atomically resolved lateral phase and amplitude contrast of the oscillation can be modeled starting from the real surface topography and taking into account the ratio of the axes of the oscillation ellipse.

The experiments were carried out on thermally evaporated 100 nm thick Au films on $LiNbO_3$ in ambient air at room temperature using a STM with mechanically machined Pt-Ir tips. The Au films were annealed at 800 °C in oxygen gas atmosphere [$p(O_2) = 1$ bar] for 30 min.[10] The flat Au (111)-terraces prepared in this way exhibited large (111) facets which were a few 100 nm wide.[11] The SAWs were excited on *Y*-cut $LiNbO_3$ with propagation in the *Z*-direction (*YZ*-$LiNbO_3$) by using interdigital transducers (IDTs). In this case the oscillation ellipse is polarized in the sagittal plane that is formed by the SAW propagation direction and the normal vector of the surface. The oscillation is described by the components u_y and u_z. The excitation frequency was 39.5 MHz, corresponding to a wavelength of 88 μm. For the comparably small scan length of about 10 nm, all the atoms are oscillating with almost the same phase, so the SAW phase delay by propagation can be neglected. The excitation level at the signal generator output was 12 dBm. As the IDT was not electrically matched, the oscillation amplitude was of the order of some parts of an Å .

The experimental problem of detecting high frequency signals by conventional STM electronics with its limited bandwidth of about 10 kHz was solved by utilizing the nonlinear tunneling curve as a frequency mixer.[12] There, the phase and the amplitude of the high frequency mechanical gap modulation are transferred, by superimposing a slightly detuned clock frequency voltage at the tunneling gap, to an easy to handle low frequency of 10 kHz.[5] The mixing additionally produces a frequency spectrum with components at the difference frequency of higher harmonics of the SAW frequency and the clock frequency[13] as well as contributions to the dc tunneling current.[14] The clock signal was chosen to 39.51 MHz at 1 V rms output voltage, while the dc sample

[a]Electronic mail: hesjedal@pdi.wias-berlin.de

 0003-6951/96/69(3)/354/3/$10.00

bias voltage was 0.6 V. The signal at the difference frequency is extracted by feeding the amplified tunneling current to a lock-in amplifier. The dc component provides the control signal for the relatively slow height feedback loop that keeps the tunneling current constant at 11.4 nA. The scans were performed with 1000×1000 data points and a collecting time per point of 100 μs. No filtering procedures were applied to the measured data.

Figure 1(a) shows the STM topography image of the hexagonal lattice structure of the Au (111) surface with a lattice spacing of approximately 5 Å . As a direct effect of ultrasound (the result does not depend significantly on the type of oscillation), we observed the smearing out of the topography image [Fig. 1(b)]. Although the atomic resolution of the topographical image vanishes, the phase signal shows a periodic distribution of structures with high contrast [Fig. 1(c)] and the amplitude shows areas of different brightness [Fig. 1(d)] at the atom positions in the hexagonal lattice. Focusing on details, the phase undergoes a contrast jump at the equilibrium position of the hexagonal lattice [Fig. 2(a)], changing from bright to dark when going parallel to the SAW's propagation direction. The measured amplitude shows an ensemble of almost hexagonal shaped rings [Fig. 2(c)]. For noise reduced amplitude images, surface adsorbates have to be avoided by measuring under ultrahigh vacuum (UHV) conditions because they strongly contribute to fluctuations of the tunneling current.[15] As generally known from wave field measurements including noise the phase is the more stable value compared to the amplitude.

In order to understand the contrast formation of phase and amplitude of the tunneling current at the difference frequency we have assumed tunneling normal to the corrugated surface, consequently being dependent on the three spherical coordinates θ, Φ, and d. For the model calculations Gaussian shape electron distributions around the hexagonal lattice positions were estimated. The wave's propagation direction is indicated by the arrow in Fig. 2(a). For a sagittally polarized oscillation trajectory and for a phase difference of the oscillation components u_y and u_z of $\pi/2$, the phase and the amplitude images are presented in Figs. 2(b) and 2(d), respectively. The ratio of the axes of the oscillation ellipse was chosen to $u_z : u_y = 0.6:1$, which is in agreement with the calculated value for YZ-$LiNbO_3$.[16] The phase and the amplitude depend on the surface topography (θ, Φ) as well as on the wave properties u_y and u_z.[5] A comparison between the experimental phase data [Fig. 2(a)] and the model calculation [Fig. 2(b)] proves the atomic phase resolution. The phase contrast reproduces the hexagonal lattice structure, and additionally, appears to be illuminated from the side. While scanning over one atom, the phase shows a relative maximum value at the point where the tunneling vector is collinear to the displacement vector, which is static for this stroboscopic measurement mode. Seen as a vector diagram, the phase is leading before passing, and retarded after passing the atom, respectively. This behavior is more drastic along the SAW propagation path than perpendicular to it. The modeled amplitude [Fig. 2(d)] shows the hexagonal shape of the reciprocal elementary lattice cell projected around the single atom with a bright maximum on the top of the atom. The measured amplitude [Fig. 2(c)] shows the hexagonal interatomic ring ensemble, but is not clearly resolving its inner structure. The difference between modeled and experimental data for the subatomic details might be due to the fact that we assumed for first calculations not a real tip geometry but a point source model.

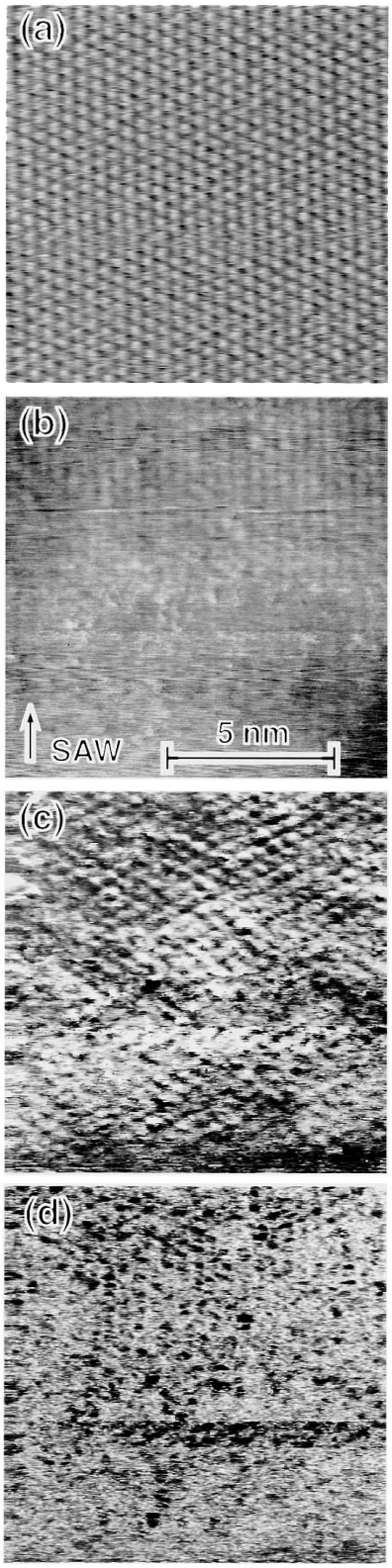

FIG. 1. Undisturbed topography image of the hexagonal Au(111) surface measured by STM (a). Topography showing reduced contrast (b), atom-resolved phase (c), and amplitude (d) measured simultaneously by SATM.

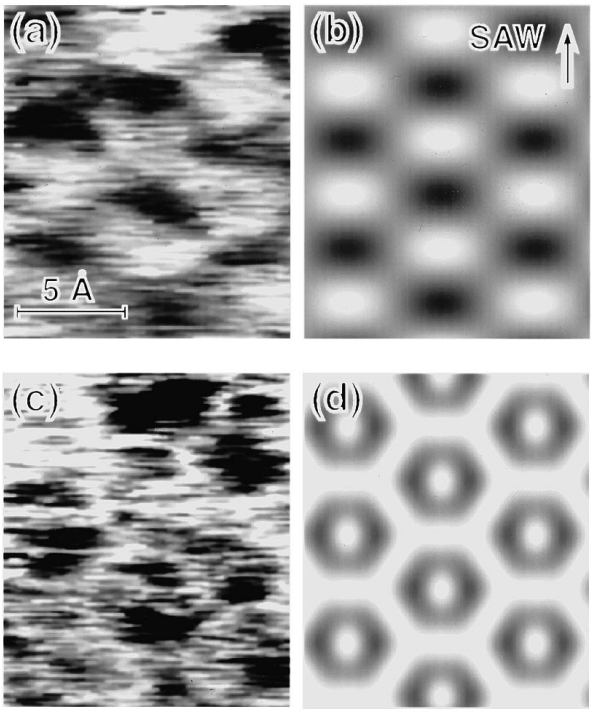

FIG. 2. Comparison of the measured (a) and (c) with the modeled (b) and (d) phase and amplitude, respectively, showing atomic resolution. The arrow in (a) indicates the SAW propagation direction.

Besides the measurement of the normal particle displacement, the determination of the in-plane component is highly desirable for a local material parameter analysis of elastic parameters. Optical probing in reflection is possible for nonvanishing normal displacement components only. In optical transmission probing an in-plane component will modulate the index of refraction together with the other oscillation components and will therefore make a separation of the different contributions difficult.[17] For the investigated Rayleigh-type SAWs the ellipse's axis ratio ranges from approximately 0.6:1 ($Au/LiNbO_3$) to 0.8:1 ($CuPC/LiNbO_3$).[18] With this variation of the constants the reconstruction of the oscillation trajectory out of the atom-resolved phase data only is almost impossible, since there is a very small variation in shape of the calculated phase curves. For greater differences in the oscillation constants in case of non-Rayleigh type SAWs, like quasi-shear polarized pseudo-SAW modes or the recently found quasi-longitudinally polarized high-velocity pseudo-SAW[19] with large in-plane oscillation components, a satisfying reconstruction just by phase measurements could be performed. In UHV measurements, the improved amplitude data will open the field of nm-size quantitative subsurface structure characterization when additionally reducing the applied SAW wavelength.

In summary, we have measured hexagonal oscillation signals with atomic resolution although the atomic topography is smeared out and the contrast is reduced due to ultrasound excitation. We obtained the atomic phase and amplitude resolution by recording stroboscopic snapshots of defined oscillation conditions with a SATM. The phase and the amplitude signal of the state of oscillation can be modeled starting from the undisturbed topography and assuming the atomic scale elliptical trajectories of a propagating SAW, which are determined by the material parameters of the surface, especially by the elastic constants. In order to reconstruct the oscillation ellipse from the experimental data including the oscillation amplitude, UHV measurements have to be performed. Since in the last years SAW frequencies of more than 10 GHz can be excited, wavelengths in the nm range are in reach. This means that even nm size structures, like quantum dots and wires, located in subsurface regions will influence the oscillation ellipse's shape due to the reduced information depth, and in reverse by calculating the axis ratio the elastic constants of those small structures become accessible.

The authors gratefully acknowledge the EC for supporting this work.

[1] G. Binning, H. Rohrer, Ch. Gerber, and E. Weibel, Phys. Rev. Lett. **49**, 57 (1982).
[2] J. Heil, J. Wesner, and W. Grill, J. Appl. Phys. **64**, 1939 (1988).
[3] S. J. Stranick, P. S. Weiss, A. N. Parikh, and D. L. Allara, J. Vac. Sci. Technol. A **11**, 739 (1993).
[4] W. Mizutani, B. Michel, R. Schierle, H. Wolf, and H. Rohrer, Appl. Phys. Lett. **63**, 147 (1993).
[5] E. Chilla, W. Rohrbeck, H.-J. Fröhlich, R. Koch, and K. H. Rieder, Appl. Phys. Lett. **61**, 3107 (1992).
[6] A. Moreau and J. B. Ketterson, J. Appl. Phys. **72**, 861 (1992).
[7] K. Takata, T. Hasegawa, S. Hosaka, S. Hosoki, and T. Komoda, Appl. Phys. Lett. **55**, 1718 (1989).
[8] W. Rohrbeck and E. Chilla, Phys. Status Solidi A **131**, 69 (1992).
[9] K. Yamanaka, H. Ogiso, and O. Kolosov, Jpn. J. Appl. Phys. **33**, 3197 (1994).
[10] L. Huang, J. Chevrier, P. Zeppenfeld, and G. Cosma, Appl. Phys. Lett. **66**, 935 (1995).
[11] V. M. Hallmark, S. Chiang, J. F. Rabolt, J. D. Swalen, and R. J. Wilson, Phys. Rev. Lett. **59**, 2879 (1987).
[12] W. Rohrbeck, E. Chilla, H.-J. Fröhlich, and J. Riedel, Appl. Phys. A **52**, 344 (1991).
[13] E. Chilla, W. Rohrbeck, H.-J. Fröhlich, R. Koch, and K. H. Rieder, Ann. Phys. **3**, 21 (1994).
[14] T. Hesjedal, E. Chilla, and H.-J. Fröhlich, Thin Solid Films **264**, 226 (1995).
[15] K. Maeda, S. Sugita, H. Kurita, M. Uota, S. Uchida, M. Hinomaru, and Y. Mera, J. Vac. Sci. Technol. B **12**, 2140 (1994).
[16] A. J. Slobodnik, E. D. Convay, and R. T. Delmonico, *Microwave Acoustic Handbook* (NTIS, Springfield, VA, 1973), Vol. 1.
[17] G. I. Stegeman, IEEE Trans. Sonics Ultrason. **SU-23**, 33 (1976).
[18] In case of Rayleigh waves and isotropic substrates, the ratio of the elastic constants c_{44}/c_{11} that can be calculated from the measurement of u_1/u_3 ranges from approximately 0.14 for Au to 0.42 for CuPC, where u_1 and u_3 are the longitudinal and the normal components of the particle displacement, respectively.
[19] M. P. Pereira da Cunha and E. L. Adler, IEEE Trans. Ultrason. Ferroelectr. Freq. Control **UFFC-42,** 840 (1995).